

# Array of micro multijunction solar cells interconnected by conductive inks

Norman Jost<sup>a,\*</sup>, Steve Askins<sup>a</sup>, Richard Dixon<sup>b</sup>, Mathieu Ackermann<sup>c</sup>, Cesar Dominguez<sup>a,d</sup>, Ignacio Anton<sup>a</sup>

<sup>a</sup> Instituto de Energía Solar, Universidad Politécnica de Madrid, Av. Complutense 30, 28040, Madrid, Spain

<sup>b</sup> Dycotec Materials Ltd, Westlea, Swindon, SN5 7SW, United Kingdom

<sup>c</sup> Insolight SA, Lausanne, Switzerland

<sup>d</sup> ETS Ingeniería y Diseño Industrial, Universidad Politécnica de Madrid, Madrid, Spain

## ARTICLE INFO

### Keywords:

Micro-CPV  
Multijunction solar cells  
High-throughput interconnection  
Conductive printing  
Screen printing

## ABSTRACT

Micro-concentrator photovoltaics (micro-CPV) consists of the reduction in size of the components of the conventional concentrator photovoltaic (CPV) technology, attaining equally high efficiencies and reducing material costs and manufacturing costs. In this publication we focus on the implementation of high throughput manufacturing methods for the interconnection of solar cells. The goal is to enable large area interconnection of thousands of micro-solar cells with a low cost of 3 €/m<sup>2</sup>. A first prototype was manufactured, interconnecting multiple 1 mm<sup>2</sup> solar cells via directly printing onto the front contact pads. The result is a glass substrate, with a size of 190 × 145 mm<sup>2</sup>, with a fully printed circuit interconnecting 12 rows each containing 11 multijunction solar cells in parallel. The fill factor (*FF*) of the full board is 76% at 214 suns.

## 1. Introduction

Micro-concentrator photovoltaics (micro-CPV) [1] is a recent development within the concentrator photovoltaic (CPV) technology [2]. The reduction in size of the solar cells and optics reduce material usage and permits high throughput parallel manufacturing methods maintaining high module efficiencies at a low cost. In addition, the smaller size permits the integration of the tracker in the module, which can then be installed in a fixed structure such as any other flat-plane photovoltaic (PV) module [3].

To guarantee the overall reduction in cost compared to conventional CPV, high throughput manufacturing methods must be adapted to the needs of the industry. A major concern is the necessary alignment precision between the solar cells and the optics and tight tolerances involved. This tolerance depends on the size of the lens-solar cell pair and ranges from 10 to 100 μm. For the precise assembly and interconnection of the dies. Cross-links with other industries can be found such as for light emitting diodes (LED) for illumination or TV screens [4]. Inspired in the solutions in these fields, we have developed and proofed a concept for interconnecting arrays of micro-solar solar cells, aiming at a cost of 3 €/m<sup>2</sup>.

This work was completed in collaboration with two companies, Insolight SA as the end user manufacturing the micro-CPV modules, and

Dycotec Materials Ltd. for the development of the necessary materials for the interconnection. Insolight is currently industrializing an integrated tracking micro-CPV module with two variants [3]. One, a hybrid approach combining CPV optics and high efficiency III-V cells for the conversion of the DNI with a backplane integrating silicon cells to collect the diffuse irradiance (Fig. 1A). A second approach, without the silicon cells results in a translucent module where the diffuse part can be used for other applications, such as growing crops in agrivoltaics applications or lighting in building integration (Fig. 1B). In the translucent module, the high efficiency multijunction solar cells are mounted on a transparent backplane to transmit the diffuse light.

Currently, the material for the multijunction cell plane is glass, but other transparent materials such as PC, or PET would also come in question for cost reduction. Insolight is looking for an interconnection method which is easily adaptable to different substrate materials. For this, a requirement is a low temperatures process which will not harm the substrate or solar cells.

The conventional method used in CPV is wire bonding. Due to the large size of the modules the solar cells are soldered and wire bonded on singular printed circuit boards (PCB) or even directly on a thermal spreader made of copper. These boards are then positioned and assembled on a large back plane and adhered again with thermally conductive adhesive, then cables are soldered for the serial or parallel connection of

\* Corresponding author.

E-mail address: [norman.jost@upm.es](mailto:norman.jost@upm.es) (N. Jost).

<https://doi.org/10.1016/j.solmat.2022.111693>

Received 23 November 2021; Received in revised form 23 February 2022; Accepted 2 March 2022

Available online 16 March 2022

0927-0248/© 2022 The Authors. Published by Elsevier B.V. This is an open access article under the CC BY-NC-ND license (<http://creativecommons.org/licenses/by-nc-nd/4.0/>).

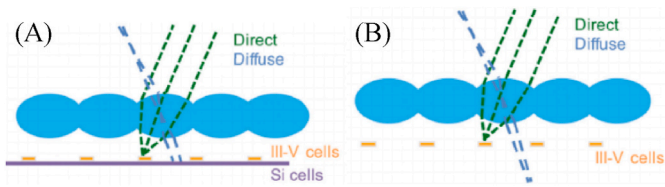


**Fig. 1.** Drawings of the two Insolight micro-CPV module types with integrated tracking, (A) with a hybrid CPV-flat plane PV approach and (B) semi-transparent for other applications such as agrivoltaics. Images from Ref. [3].

each board [5]. For the conventional CPV technology this was a viable option, as modules with a dimension of  $1 \text{ m}^2$  would have ca. 600 solar cells with  $40 \times 40 \text{ mm}^2$  lenses. In many cases they have even fewer solar cells, in the range of 40 cells/ $\text{m}^2$  if the lenses are bigger ( $160 \times 160 \text{ mm}^2$ ). In the case of the micro-CPV setting, e.g. Insolight, the modules contain over 5000 solar cells/ $\text{m}^2$  [3]. The conventional wire bonding method is prohibitive due to the number of dies and the required precision throughout large areas [1].

An alternative approach is based on Surface Mount Technologies (SMT), the chip-on-board (COB) approach which is widely applied in the LED lighting industry [6,7]. The solar cells are encapsulated and electrically connected on surface mount devices where a Secondary Optical Element (SOE) can be directly overmolded [8]. Large planes are then populated with these small chips by pick-and-place and reflow soldering or gluing for the adhesion and electrical connection. For now, this is the only commercially viable option.

The challenge of interconnecting solar cells has also been addressed with another method which has been used for LEDs and solar cells before. The method consists of the evaporation of gold or other precious metals for the interconnection [9], this method is elaborative having to use a lithography step and comes with a great loss of gold or other metals for large areas. Another, more viable approach, is the use of custom solar cells with both contacts on one side. This has been experimentally proven [10]. Problems with this solution is the elaborative custom solar cells, bringing both contacts on one side complicates the manufacturing. Cells as such are currently not commercially available.

The objective of the work is the development of a process to adhere and contact the bare solar cells on a large plane with a few simple steps. The process would be compatible with mass population technologies with very high precision, the proven fluid self-assembly (FSA) ( $<1 \mu\text{m}$ ) [11,12] and the already applied in industry, chiplet printing ( $5\text{--}10 \mu\text{m}$ ) [13]. Once the solar cells are populated on the plane the interconnection is an issue. The current way for interconnecting the front contact pads would be wire bonding, yet this approach is not viable due to the large quantity of dies on such a large area, cost estimation resulted in prices of  $\text{€}500/\text{m}^2$ . An alternative is proposed with this concept, instead of using wire bonds we directly print conductive silver ink onto the front pads for the interconnection. A similar approach has been presented before for the interconnection of LED dies [14].

Different printing technologies are suitable for our direct printing interconnection method (DPIM), such as syringe printing, jet printing [14] and serigraphy/screen printing. During this project the first attempts with single solar cells were completed with syringe printing [15] and later screen printing was used for the full board. Conductive materials used are low-cost silver inks with a sheet resistance of  $9.7 \text{ m}\Omega/\square$ , these inks were synthesised by Dycotec to tune the viscosity for an optimum printing resolution. The combination of these cheap silver inks and the cheap screen printing process could bring the cost down to  $3 \text{ €}/\text{m}^2$  for this technology. This value is estimated by Dycotec taking into account the cost of the silver inks and the screen printing process for  $1 \text{ mm}^2$  solar cells with a quantity of 5000 dies/ $\text{m}^2$ . Assembly of the solar cells is not included in the estimation.

An unavoidable requirement for the front contact of cells with conductive inks is the electrical insulation of the lateral perimeter of the

solar cells to avoid short circuiting. The ideal solution would be to use solar cells, which are electrically insulated during the manufacturing process of the dies by depositing the anti-reflective (AR) coating or other insulation material on the sides of the cells such as shown by Ref. [16]. Yet, no solar cell manufacturer has this technology implemented in their production line, so this option was currently not possible.

As an alternate solution,  $1 \text{ mm}^2$  inverted metamorphic triple-junction (IMM) solar cells were used for the most recent trials. This solar cell technology has a low thickness of  $30 \mu\text{m}$ , making the insulation with syringe printing possible. The solar cells have two contact pads on the front side each with  $100 \times 100 \mu\text{m}^2$  used for the directly printed interconnection and wire bonds for comparison.

The primary goal of the method shown in this publication is to show a viable alternative to wire bonding without any significant losses in fill factor (*FF*) for single cells and a full board at an operating concentration of 200X which represents the current specification of the Insolight modules and a representative case study for micro-CPV applications.

## 2. Direct silver ink printing interconnection method

The proposed direct printing interconnection method (DPIM) uses two materials for the front connection, an epoxy dielectric for the insulation of the lateral of the solar cell to avoid short circuiting and the conductive silver ink which is printed over the front contact pads of the solar cells to the tracks on the glass plane. A schematic of this approach is shown in Fig. 2.

The step by step for the DPIM of the solar cells would be as follows:

1. Screen printing of the interconnection tracks on the glass board and curing at temperatures slightly over  $100 \text{ }^\circ\text{C}$
2. Pick-and-place of the solar cells and reflow soldering for the electrical contact and adhesion
3. Dielectric syringe printing around the solar cells for electrical insulation of the solar cell lateral and ultraviolet light curing of the dielectric. This step would be disposable if dies are electrically insulated
4. Screen printing of the final interconnection layer with epoxy silver ink and temperature curing

As seen this method consists of only a few steps without using any further components but the transparent substrate, the solar cells, and the inks. Step 3 can be avoided if the lateral insulation of the dies is achieved during the manufacturing of the cells, the process would be even more simplified with less equipment needed.

The challenges with DPIM are first, the successful insulation of the lateral of the solar cell; and second, the perfect alignment of the screen with the solar cell plane. The area of the contact pads designed is only  $100 \times 100 \mu\text{m}^2$ , which leads to very tight tolerances for the screen printing of  $20 \mu\text{m}$ . This tolerance is acceptable for guaranteeing a good ohmic contact between the silver ink and pads, and for avoiding too much shading of the active area of the solar cell. Screen printing on large scales allows for line-widths of  $70 \mu\text{m}$  [17]. For smaller devices up to  $500 \mu\text{m}$  in side ( $50 \mu\text{m}$  pads) with the same front metallization layout, this method is still applicable but with considerable shading loss. It would be beneficial to change the layout for a single contact area, e.g. a

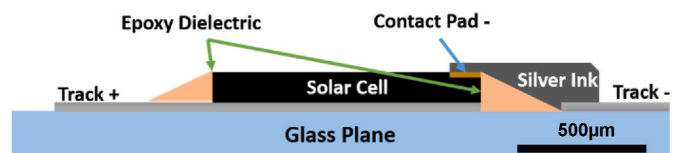


**Fig. 2.** Schematic of the finished interconnection. The dielectric surrounds the solar cell to insulate and avoid lateral shunting. The silver ink interconnects the solar cell with the glass plane tracks.

larger bus bar. If the requirement is to use even smaller solar cells <500 μm, screen printing would be difficult to implement. Either a more precise printing technologies would have to be used [17], or the front metallic layout of the solar cell has to leave the necessary area for DPIM [16], accepting the reduction of active area.

### 3. Full board prototype

The prototype developed consist of 190 × 145 mm<sup>2</sup> glass board manufactured with the steps described in section II. The full board has 143 cells arranged in 13 rows. 12 rows are connected in series, each row has 11 cells connected in parallel (see Fig. 3). These 12 rows are measured when referred to full board measurements. There are no bypass diodes for this design, later iterations of the board will include them. The remaining row (13th) is for test purposes, it has single interconnected solar cells (Fig. 3). The single cell measurements in this publication are of the best performing solar cell of this row. The size of this prototype boards corresponds to 1/58 of the current 1.6 × 1 m<sup>2</sup> micro-CPV solar modules from Insolight. This size was limited by the available equipment but is representative enough to demonstrate the process for a later scale-up in a production line.

Manufacturing of the full board prototype is as follows. First, the glass board was cleaned from residues. The silver ink tracks, and both top and bottom contact pads are printed via screen printing. The corners of the glass board are used for alignment of the screen. Once thermally cured, the 1 mm<sup>2</sup> solar cells are positioned with a pick & place and soldered onto the pads. Right after soldering, syringe printing is used to deposit the epoxy dielectric for the lateral insulation of the cells. After thermal curing, the DPIM is completed by a second screen printing of the silver ink contact layer, the alignment of the screen is guaranteed by using the edges of the glass board again (alignment is in the range of 20 μm).

An electroluminescence of the full board (see Fig. 4) shows 10 out of 12 rows lighting up correctly. Due to the novelty of the process for this scale, errors in the process caused some rows to be short-circuited. The short circuiting happened on cell level, with imperfect lateral insulation.

The adhesion on glass for the silver ink tracks is sufficient and the same material is currently being used for the Insolight modules

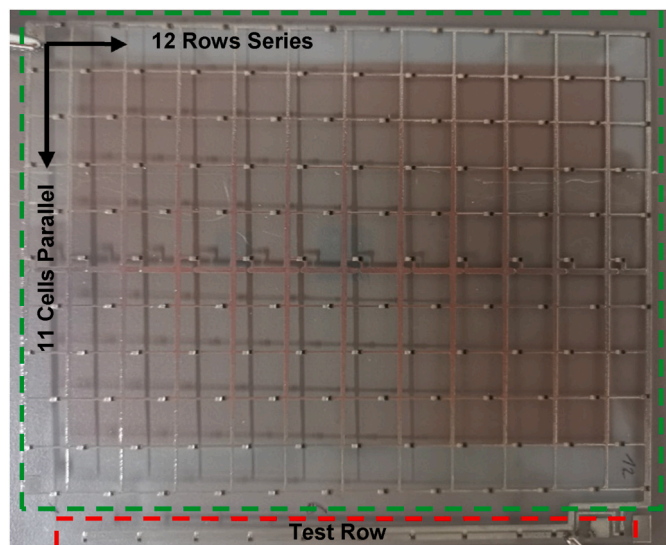


Fig. 3. Image of the full board of 143 solar cells, the spacing of the cells is suitable for Insolights hexagonal lens arrays. It has 1/58 of the size of the current modules. 12 rows are interconnected in series with 11 cells in parallel (surrounded by green dashes). One test row is composed of single solar cells separated from the rest (red dashes). (For interpretation of the references to colour in this figure legend, the reader is referred to the Web version of this article.)

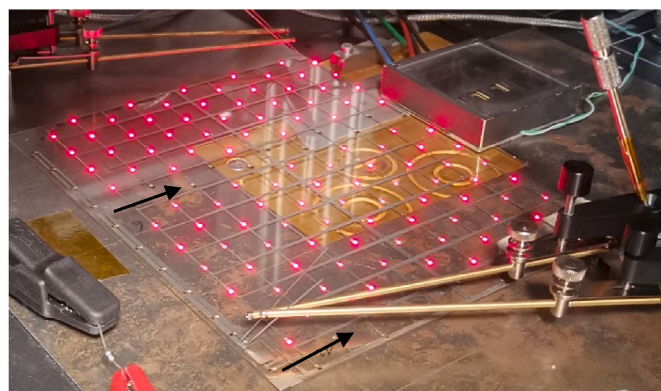


Fig. 4. Electroluminescence image of the full board. 10 rows which emit light, meaning 10 of the 12 rows are properly interconnected. The missing two rows are marked with black arrows. The image was taking in the setup for measuring IV under concentration SAV Helios 3030.

backplane layout. These prototypes have been extensively thermal cycled without any failure of the screen printed silver tracks.

#### 3.1. Electrical characterization of single cells on board

Single solar cells on the board with good electroluminescence were selected. These solar cells were electrically characterized measuring dark-IV and the IV under concentration. Simultaneously we measured a good performing single IMM wire bonded solar cell as a benchmark.

##### 3.1.1. Dark-IV of single cells

With the same set-up and conditions. The wire bonded solar cell uses Ø25 μm gold wire and three bonds. Fig. 5 shows the measured dark-IV curves. The series resistance is lower for the in this paper presented DPIM, this good result is also confirmed by the measurements under concentration which follow this section. It must be pointed out that these thin and flexible IMM solar cells are not designed for wire bonding, so a poor contact resistance between wires and pads was expected. Nevertheless, single IMM cells with a printed interconnection achieved comparable results to single UMM (Upright Metamorphic) cells designed for wire bonding as shown in the proof-of-concept publication [15]. In Fig. 6A the wire bonded IMM solar cell can be seen under EL, and in Fig. 6B a very good attempt of interconnecting using DPIM with minimal shading losses.

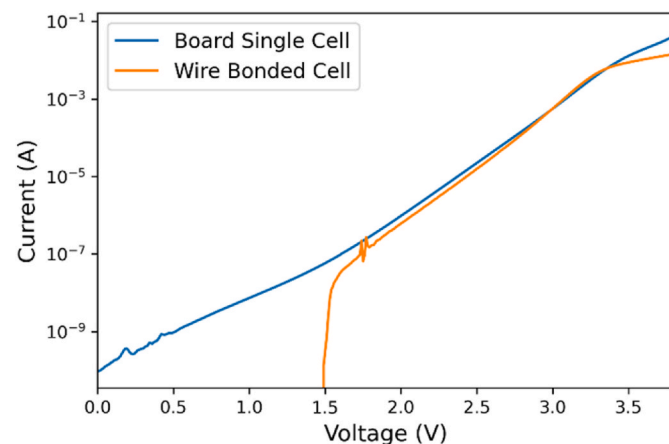


Fig. 5. Dark-IV of the singulated solar cell and one wire bonded solar cell of the same technology. The series resistance is present but lower for the singulated cell with the novel interconnection method seen by different slopes at higher voltages.

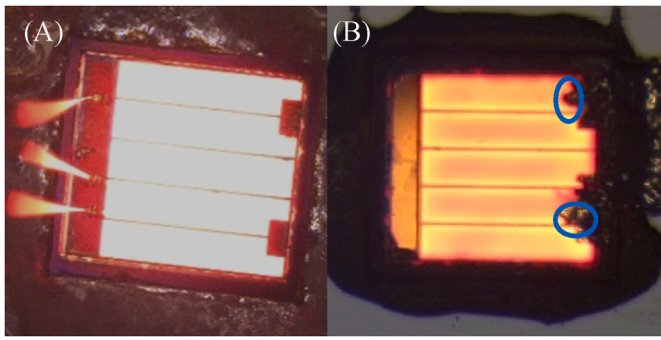


Fig. 6. Single inverted metamorphic solar cells, (A) is a correctly wire bonded cell and (B) a very good by screen printing interconnected solar cell with minimal shading caused by spillage of the conductive ink over the active area of the solar cell (encircled in blue). (For interpretation of the references to colour in this figure legend, the reader is referred to the Web version of this article.)

### 3.2. Concentrated light-IV of single cells

We measured and compared the IV curves under concentration for the singulated 1 mm<sup>2</sup> IMM cell with the DPIM (Fig. 7A) and an IMM cell

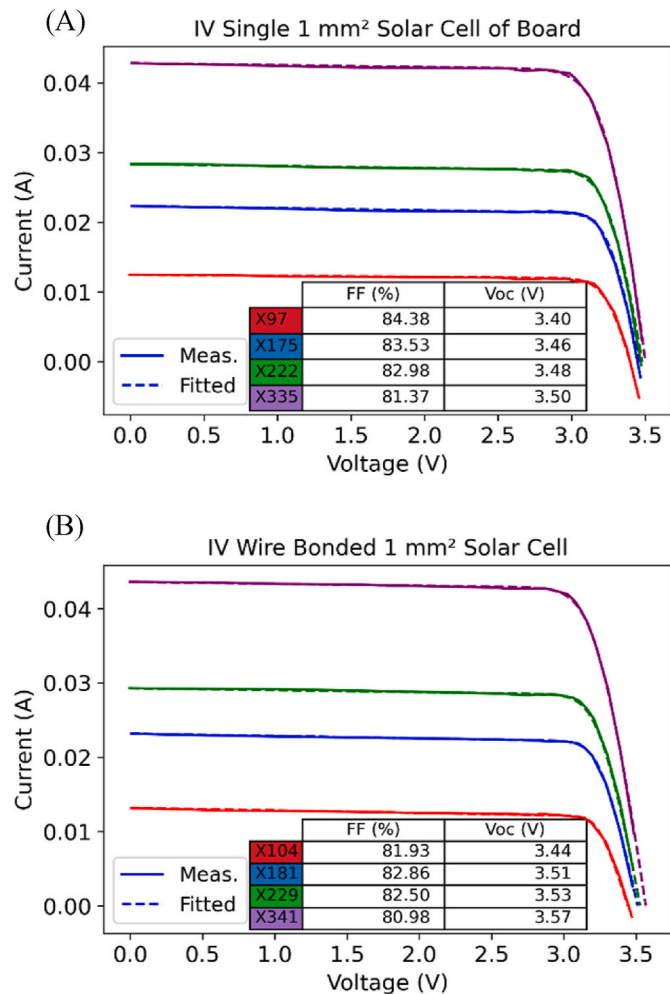


Fig. 7. (A) Best performing single solar cell solar cell IV curves under different concentrations. The table collects the concentrations and fill factors. (B) Best performing wire bonded single solar cell. Comparing to (A) the fill factors are ca. 1 percentage point lower and specific series resistance is slightly higher with 72 mΩcm<sup>2</sup> vs. 54 mΩcm<sup>2</sup> at 220X. This is due to difficulties wire bonding these novel and very fragile 1 mm<sup>2</sup> large and 30 μm thick flexible IMM solar cells.

from the same wafer encapsulated and connected using wire bonds (Fig. 7B). The same solar cells as measured in part 3.1.1 Dark-IV. Each figure includes one diode fits for the IV-curves at different concentrations.

Light IV measurements are done with a Solar Added Values S.A. Helios 3030 CPV simulator. Different concentrations are achieved by changing the distance between the xenon flash lamp and device under test. The sample is kept on a cooling plate at 25 °C. The spectrum is controlled using isotype solar cells, which have a very similar external-quantum-efficiency as the top two junctions of the IMM solar cells. The spectral matching ratio (SMR) [18,19] quantifies a particular irradiance spectrum by comparing it with the reference spectrum AM1.5D [20]. Providing a methodology to assure the same current mismatch between the subcells [21] under both irradiance spectra when SMR equals 1.0. The SMR for the top and middle subcell is 1.0 at the reference concentration ratio (222 suns in Fig. 7A). An inverted grown GaAs isotype solar cell was used to determine that there is no current limitation for the bottom subcell during the measurement. This subcell operates with a slight excess current. The resulting IV-curves can be seen in Fig. 7. The effective concentration is determined by the ratio of measured and specified I<sub>SC</sub> calculated from the short circuit current density (J<sub>SC</sub>) measured by the manufacturer at one sun (10.95 mA/cm<sup>2</sup>). One diode fits are used to calculate the series resistance (R<sub>s</sub>) and the fill-factor (FF). The FF is also included in the table of each figure. For better comparison the R<sub>s</sub> is converted to the specific series resistance (r<sub>s</sub>). The fitting is done using pvlb for python (F [22]).

The series resistance for the DPIM is lower than the wire bonded case with a specific r<sub>s</sub> of 54 mΩcm<sup>2</sup> vs. 72 mΩcm<sup>2</sup> at ca. 220X. The fill factor reaches 83.5% for the cells with the novel interconnection method at a concentration of 175X. This is very close to the resulting FF of IVs measured by the manufacturer using probes while the cells were still on the donor substrate, the mean FF is 84.0%.

For the single cell, the result is better than the wire bonded case. As mentioned before, these solar cells are not optimized for wire bonding and very delicate due to their thickness. A comparison with another solar cell type can be found in Ref. [15]. Yet, it should be taken into account that wire bonding is currently the only industrial alternative for the interconnection of CPV solar cells and that wire bonding is known to cause damage to delicate devices such as these [23]. Due to this, the DPIM is an alternative for these types of devices. The result shows that direct silver ink printing method can reach good results with screen printing on a single cell level. Now we proceed with the measurement of the full board.

### 3.3. Electrical characterization of the full board

#### 3.3.1. Dark-IV measurement of the full board

The dark IV of the full board was measured on a cooling plate keeping the temperature at 25 °C, see Fig. 8. The IV curve shows a linear slope at high voltages which is due to R<sub>s</sub>. Fitting the curve with a one diode model gives a value for r<sub>s</sub> of 67 mΩcm<sup>2</sup> at current values over 300 mA (equivalent resistance value) which can potentially provide a FF over 80% at the nominal concentration of 200X. A similar resistance value is extracted in the next section (concentrated light IV) and further discussed there.

#### 3.3.2. Concentrated light-IV measurement of the full board

The same Helios 3030 simulator is used for the full board measurements. The simulator had to be modified by adding higher range alimentation sources to reach the V<sub>OC</sub> of the board.

Fig. 9 shows the IV curves of the full board under the intended concentration of 214X, it is fully operative. Nevertheless, the performance of the full board is significantly lower (FF = 76%) compared to the single cell shown in the previous section (FF = 83%). In addition to this, we can also see that the open circuit voltage is not the same as expected. We measured a V<sub>OC</sub> of 32.4 V, a single cell has 3.5 V at around

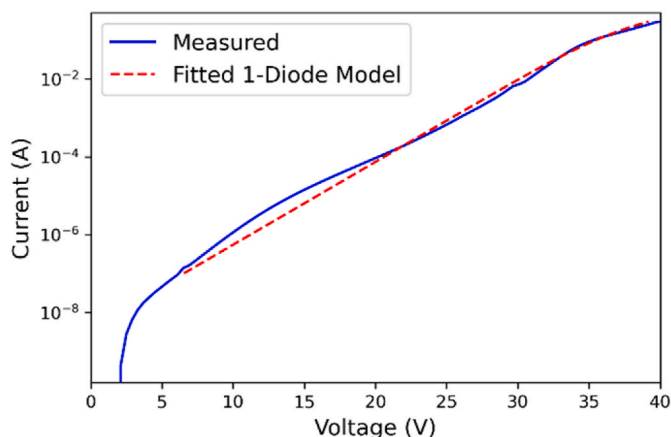


Fig. 8. Dark-IV curve of the full 12 × 11 solar cell board, showing a specific series resistance of 67 mΩcm<sup>2</sup> in the high current area which corresponds to concentrations of 200–300 suns.

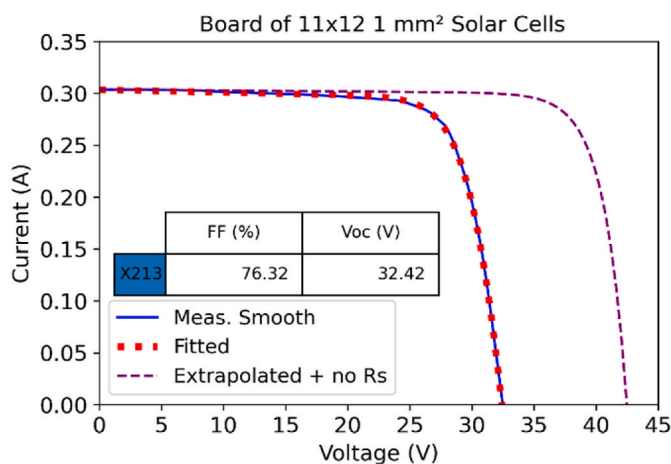


Fig. 9. Full board IV curve measurement at a concentration of 214X. With a measured  $V_{OC}$  of 32.42 V and a fitted  $R_S$  of 5.00 Ω for 214X. The fill factor is of 76.3%, 6 percentage points lower than for the single solar cell. The dashed purple curve shows a fit with the fill factor (83%) from the single cell measurement (Fig. 7) and an expected  $V_{OC}$  of 42.5 V (single solar cell  $V_{OC}$  × 12 rows). This is the current potential for the IV curve of the full board without any manufacturing problems. (For interpretation of the references to colour in this figure legend, the reader is referred to the Web version of this article.)

220X. This results in 9 out of 12 rows functioning correctly. This is caused by problems during the solar cell assembly on the board. Cracked cells leading to shunts as revealed by visual and EL inspection in the next section (3.4). As well as, bad perimeter insulation leading to short circuiting of single cells in a row. The resulting equivalent  $r_S$  is 46 mΩcm<sup>2</sup> at 214X. The value is close to the previously extracted value from the dark-IV measurement (67 mΩcm<sup>2</sup>) and is similar to the one measured for a single solar cell on the board 54 mΩcm<sup>2</sup>, proving that the resistance is not an issue in the performance of the full board. In Fig. 9 we also added an IV-curve (dashed purple) which shows us the potentials result without any manufacturing issues, a FF of 83% and  $V_{OC}$  of 42.5 V.

### 3.4. Visual inspection of the full board

Images under the microscope were taken to inspect the tracks, interconnects and solar cells. It is to be noted that this is the first prototype board of its kind to be manufactured with a novel interconnection method and the assembly of the board was made by a semi-manual process.

As already shown in sections before not all the rows were properly interconnected (Fig. 4). Two of the 12 rows don't light up in EL and the  $V_{OC}$  of the full board shows a voltage value for 9 rows instead of 12. The tracks are neatly printed as seen in Fig. 10A, without any discontinuations. The measured specific series resistances are also very similar between the full board and single cell measurements, pointing out that the resistance is not a problem. Nevertheless, a few cells were not properly insulated and are short circuited by the conductive inks. The insulation resistance for functioning rows is around the MΩ mark.

Microscope EL-images reveals also partial shading in some cells due to overflow of the dielectric and non-perfect alignment of the printed silver ink which not only covers the contact pads but also active areas of the solar cell (Fig. 10B–D). This misalignment is caused by insufficient precision in the placement of the solar cells, some are rotated causing misalignments up to 100 μm, see Fig. 10C. With the contact pad size of 100 × 100 μm<sup>2</sup>, such a misalignment causes the near missing of the pads when using the DPIM. An acceptable misalignment would be in the range of 10 μm, or even lower which could be achieved with fluid self assembly [11] or chiplet printing [13].

The EL-images also show cracks in some cells (Fig. 10B). The 30 μm thin and fragile 1 mm<sup>2</sup> solar cells come adhered on a thermal tape. Even when released, static force causes the cells to stick on the tape. A vacuum nozzle is used to lift the solar cells from the tape, sometimes excessive force had to be applied to release the cells. Also, during the pick & place of the thin solar cells it is easy to apply too much pressure and cause cracking. Most cells (~80%) show cracking in the center where the nozzle touches the surface.

Being the first prototype board of its kind to be manufactured with a novel type of fragile solar cells these kinds of problems were to be expected. To avoid these cracks more experience needs to be gained on how to handle these ultra-thin solar cells which are the first of their kind for micro-CPV. Different populating mechanism as described in the introduction such as chiplet printing or fluid self-assembly could help to avoid such damages. The misalignment of the solar cells of up to 100 μm (Fig. 10C) was caused due to a 30% over dimension of the pads, making a precise manual placement of the cells difficult. With the correct pad dimension and an automatized placement of the cells this would be

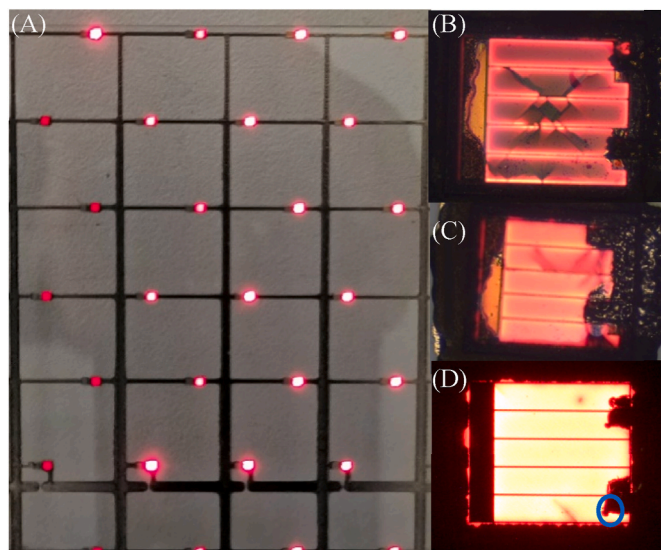


Fig. 10. (A) Shows a close-up of a functioning section of the board under EL-emitance. A good screen printing of the conductive tracks is seen. Microscope EL images of cells (B–C), in which cracking and surface damages of the solar cell can be seen in (B–C), (D) shows a perfectly functioning solar cell. In (B–C) misalignments of the screen printed interconnects can be seen. In (D) the alignment is good but a little overflow of the silver ink can be seen (circled in blue). (For interpretation of the references to colour in this figure legend, the reader is referred to the Web version of this article.)

avoided.

Results show a working interconnected board under concentration with a good performance at the intended concentration of ca. 200X. The difference in specific series resistance ( $r_s$ ) between the full board 46 m $\Omega$ cm<sup>2</sup> and the single cell 54 m $\Omega$ cm<sup>2</sup> at the concentration of 220X (Fig. 7AB) is minimal. This is consistent with the good sheet resistance of the silver inks of 9.7 m $\Omega$ /□. The FF of the full board is 76%, significantly lower than the FF achieved with the single interconnected solar cell 83%. This loss is mostly caused by cracking of solar cells on the full board and short-circuited rows. With a few improvements in the process at least the same FF should be in reach for the whole board (83%). The scale of the board is also still small reaching only 1/58 of the full area of the Insolight SA. module, this is to be increased in future tests.

#### 4. Conclusion

A first fully printed board with 132 interconnected multijunction solar cells shows a good result at the intended concentration of 200–220 suns. Yield of the process must be improved with unwanted shunts caused by cracking of the very thin and fragile inverted metamorphic cells and short circuiting due to bad lateral insulation. Yet, it is shown that the silver inks permit for a very good series resistance tough visible misalignments in the placement of the cells and printing process. An important step has been made towards a very economic (goal of 3€/m<sup>2</sup>) high throughput manufacturing method for interconnecting micro-CPV solar cells. Giving an alternative to a high cost wire bonding technology on high cell density micro-CPV modules or a more material intensive chip-on-board solution. A fill-factor (FF) of 76% with a  $V_{OC}$  of 32.4 V for the 12 × 11 cell board at a concentration of 214 suns was measured. A single solar cell on the board reached a FF of 83.5%, very close to the 84% given as specification from the manufacturer (one-sun measurement). This FF shows the potential of what is achievable with the full board in future experiments. Future research will also seek the limit of screen printing for cells with 500 μm in side and even smaller solar cells using other printing technologies which permit thinner line widths.

#### CRedit authorship contribution statement

**Norman Jost:** Investigation, Methodology, Visualization, Writing – original draft, Writing – review & editing. **Steve Askins:** Project administration, Methodology, Investigation, Funding acquisition, Conceptualization. **Richard Dixon:** Funding acquisition, Investigation, Methodology, Project administration. **Mathieu Ackermann:** Project administration, Methodology, Investigation, Funding acquisition. **Cesar Dominguez:** Methodology, Funding acquisition. **Ignacio Anton:** Writing – review & editing, Methodology, Investigation, Funding acquisition.

#### Declaration of competing interest

The authors declare that they have no known competing financial interests or personal relationships that could have appeared to influence the work reported in this paper.

#### Acknowledgements

The ENabling Micro-ConcEntrator PhotovoltaicS with Novel Interconnection Methods (ENMESH) project is supported under the umbrella of ERA.NET Cofund by MINECO under the reference PCI2018-093168, Innovate UK and Swiss Federal Office of Energy. Norman Jost is funded via the grant FPI (Ref. PRE2018-085913) from the project ENE2017-87825-C2-1-R by the MCIN/AEI/10.13039/50110001103 and by ERDF “A way of making Europe”.

Jesus Bautista for the wire bonding and Manuel Hinojosa for helping with the interpretation of the dark-IV measurements.

#### References

- [1] C. Domínguez, N. Jost, S. Askins, M. Victoria, I. Antón, A review of the promises and challenges of micro-concentrator photovoltaics, AIP Conf. Proc. 1881 (1) (2017), 080003, <https://doi.org/10.1063/1.5001441>.
- [2] M. Wiesenfarth, I. Anton, A.W. Bett, Challenges in the design of concentrator photovoltaic (CPV) modules to achieve highest efficiencies, Appl. Phys. Rev. 5 (4) (2018), 041601, <https://doi.org/10.1063/1.5046752>.
- [3] G. Nardin, C. Domínguez, Á.F. Aguilar, L. Anglade, M. Duchemin, D. Schuppisser, F. Gerlich, M. Ackermann, L. Coulot, B. Cuénod, D. Petri, X. Niquille, N. Badel, A. Lachowicz, M. Despeisse, J. Levrat, C. Ballif, S. Askins, R. Núñez, I. Antón, Industrialization of hybrid Si/III–V and translucent planar micro-tracking modules, Prog. Photovoltaics Res. Appl. (2020), <https://doi.org/10.1002/pip.3387>.
- [4] K. Ding, V. Avrutin, N. Izyumskaya, Ü. Özgür, H. Morkoç, Micro-LEDs, a manufacturability perspective, Appl. Sci. 9 (6) (2019), <https://doi.org/10.3390/app9061206>.
- [5] A.L. Luque, A. Viacheslav, Concentrator photovoltaics, in: Concentrator Photovoltaics, Springer Berlin Heidelberg, 2007, <https://doi.org/10.1007/978-3-540-68798-6>.
- [6] R. Keeler, Chip-on-board technology, in: The Electronics Assembly Handbook, 1985, [https://doi.org/10.1007/978-3-662-13161-9\\_9](https://doi.org/10.1007/978-3-662-13161-9_9).
- [7] O. Kückmann, High-power LED arrays: special requirements on packaging technology, Light-Emitting Diodes: Research, Manufacturing, and Applications X 6134 (2006) 613404, <https://doi.org/10.1117/12.646321>, 2000.
- [8] H. Zheng, L. Li, X. Lei, X. Yu, S. Liu, X. Luo, Optical performance enhancement for chip-on-board packaging LEDs by adding TiO<sub>2</sub>/silicone encapsulation layer, IEEE Electron. Device Lett. 35 (10) (2014) 1046–1048, <https://doi.org/10.1109/LED.2014.2349951>.
- [9] M.P. Lumb, K.J. Schmieder, T.C. Mood, D. Balwin, W. Wagner, J.E. Moore, M. Meitl, L.B. Ruppalt, N. Kotulak, J.A. Nolde, E.A. Armour, Z. Pulwin, B.R. Fisher, J. Carter, S. Burroughs, Design, modeling, and experimental results for CPV arrays built using heterogeneously integrated III–V micro-cells, <https://doi.org/10.1117/1.2.2549037>, 2020, 1127504(March), 3.
- [10] H. Arase, A. Matsushita, A. Itou, T. Asano, N. Hayashi, D. Inoue, R. Futakuchi, K. Inoue, T. Nakagawa, M. Yamamoto, E. Fujii, Y. Anda, H. Ishida, T. Ueda, O. Fidaner, M. Wiemer, D. Ueda, A novel thin concentrator photovoltaic with micro-solar cells directly attached to a lens array, IEEE Journal of Photovoltaics 4 (2) (2014) 709–712, <https://doi.org/10.1109/JPHOTOV.2013.2292364>.
- [11] T. Fukushima, T. Konno, E. Iwata, R. Kobayashi, T. Kojima, M. Murugesan, J. C. Bea, K.W. Lee, T. Tanaka, M. Koyanagi, Self-assembly of chip-size components with cavity structures: high-precision alignment and direct bonding without thermal compression for hetero integration, Micromachines 2011 2 (1) (2011) 49–68, <https://doi.org/10.3390/MI2010049>, 49–68, 2.
- [12] M. Kaltwasser, U. Schmidt, L. Lösing, S. Biswas, T. Stauden, A. Bund, H.O. Jacobs, Fluidic self-assembly on electroplated multilayer solder bumps with tailored transformation imprinted melting points, Sci. Rep. 9 (1) (2019) 1–8, <https://doi.org/10.1038/s41598-019-47690-8>.
- [13] Y. Wang, B.B. Rupp, A. Plochowitz, L.S. Crawford, M. Shreve, S. Raychaudhuri, S. Butylkov, Y. Wang, P. Mei, Q. Wang, J. Kalb, E.M. Chow, J.P. Lu, Chiplet micro-assembly printer, in: Proceedings - Electronic Components and Technology Conference, 2019-May, 2019, pp. 1312–1315, <https://doi.org/10.1109/ECTC.2019.00203>, Figure 1.
- [14] A. Rudorfer, M. Tscherner, C. Palfinger, F. Reil, P. Hartmann, I.E. Seferis, E. Zych, F.P. Wenzl, A study on Aerosol jet printing technology in LED module manufacturing, Fifteenth International Conference on Solid State Lighting and LED-Based Illumination Systems 9954 (2016) 99540E, <https://doi.org/10.1117/12.2237737>.
- [15] N. Jost, S. Askins, R. Dixon, M. Ackermann, C. Dominguez, I. Anton, Novel interconnection method for micro-CPV solar cells, Conf. Rec. IEEE Photovolt. Spec. Conf. (2021) 1166–1169, <https://doi.org/10.1109/PVSC43889.2021.9518837>.
- [16] P. Albert, A. Jaouad, G. Hamon, M. Volatier, C.E. Valdivia, Y. Deshayes, K. Hinzler, L. Béchou, V. Aimez, M. Darnon, Miniaturization of InGaP/InGaAs/Ge solar cells for micro-concentrator photovoltaics, Prog. Photovoltaics Res. Appl. 29 (9) (2021) 990–999, <https://doi.org/10.1002/pip.3421>.
- [17] Q. Huang, Y. Zhu, Printing conductive nanomaterials for flexible and stretchable electronics: a review of materials, processes, and applications, Advanced Materials Technologies 4 (5) (2019) 1–41, <https://doi.org/10.1002/admt.201800546>.
- [18] N. Jost, I. Antón, R. Núñez, S. Askins, L.J.S. José, G. Vallerotto, R. Herrero, M. Victoria, C. Domínguez, G. Sala, From component to multi-junction solar cells for spectral monitoring, AIP Conf. Proc. (1) (2018) 100002, <https://doi.org/10.1063/1.5053546>, 2012.
- [19] M. Victoria, S. Askins, R. Núñez, C. Domínguez, R. Herrero, I. Antón, G. Sala, J. M. Ruiz, Tuning the current ratio of a CPV system to maximize the energy harvesting in a particular location, AIP Conf. Proc. 1556 (2013) 156–161, <https://doi.org/10.1063/1.4822221>.
- [20] R.E. Bird, R.L. Hulstrom, L.J. Lewis, Terrestrial solar spectral data sets, Sol. Energy 30 (6) (1983) 563–573, [https://doi.org/10.1016/0038-092X\(83\)90068-3](https://doi.org/10.1016/0038-092X(83)90068-3).
- [21] C. Domínguez, I. Antón, G. Sala, Multijunction solar cell model for translating I–V characteristics as a function of irradiance, spectrum, and cell temperature, Prog. Photovoltaics Res. Appl. 18 (4) (2010) 272–284, <https://doi.org/10.1002/pip.965>.
- [22] F. Holmgren, C.W.W. Hansen, M.A. Mikofski, Pvlb python: a python package for modeling solar energy systems, Journal of Open Source Software (2018), <https://doi.org/10.21105/joss.00884>.
- [23] I. Rey-Stolle, C. Algora, Analysis of wirebonding techniques for contacting high concentrator solar cells, IEEE Trans. Adv. Packag. 26 (1) (2003) 47–53, <https://doi.org/10.1109/TADVP.2003.811366>.